Id.: EN-56

CHANNEL BLOCKAGE ANALYSIS OF THE SMART REACTOR

Lucas P. C. Leão[1], Gustavo L. A. Ribeiro[1, 2], Bruno V. de Melo[1], Antonella L. Costa[1, 2]

[1] Universidade Federal de Minas Gerais, Departamento de Engenharia Nuclear - Escola de Engenharia - Bloco 4 (Av. Antônio Carlos, 6627, Campus Pampulha, 31270-90, Belo Horizonte, MG, Brazil)
[2] CNPq National Institute of Science and Technology – Modular and Innovative Nuclear Reactors, Brazil
lucaspatric@ufmg.br; gustavo9661@ufmg.br; bviotti@protonmail.com; antonella@nuclear.ufmg.br

Keywords: SMART reactor, Heat Flow, Coolant Redistribution, Crossflow, RELAP5

ABSTRACT

In recent times, the attractiveness of small modular reactors (SMRs) has been increasing due to their lower construction and operational costs, more versatile positioning and distribution, among other advantages in comparison to large-size power plants. A particularly relevant SMR is the System Integrated Modular Advanced Reactor (SMART), developed by the Korea Atomic Energy Research Institute (KAERI). The SMART reactor integrates major components inside a single reactor pressure vessel, simplifying the coolant flow circuit, maintenance and, in particular, helping to reduce the risk of channel blockage. Nevertheless, other common causes for flow blockages persist and their potential effects must be evaluated. In this context, this paper aims to analyze the effects of a core channel blockage transient during normal operation of the SMART reactor's core and the safety mechanisms implemented to address these issues, validating the structural advantages of this reactor. Furthermore, the results of this transient considering the core modeling with and without cross flow between the channels was considered. The simulation of the core and the primary flow circuit was conducted using the RELAP5 computer code, incorporating standard literature data for the reactor. The analysis of the results provides insights into the reactor's safety levels and highlights potential challenges to achieving the desired long operational lifetime of the structure.

1. INTRODUCTION

The SMRs are nuclear reactors with a total power capacity up to 300 MW(e) per unit and are also characterized by their compact designs and simpler manufacturing, transport, and implementation of components when compared to traditional nuclear reactors [1]. The SMRs also display passive safety systems that increase the overall safety of the power plant. These aspects have made SMRs viable commercial alternatives to nuclear power and several projects of this type have been developed in the last decades [2].

Among the SMRs is the System Integrated Modular Advanced Reactor (SMART) developed by the Korea Atomic Energy Research Institute (KAERI) [3][4], which was the first licensed integral-type reactor in history [5]. The major components of the SMART reactor are contained in a single reactor pressure vessel (see Figure 1 (a)), and its safety is enhanced by the single-structure design and complemented by various safety systems, such as the safeguard vessel, an emergency core cooling system and a passive residual heat removal system [6].

The SMART reactor core under study is composed of 57 fuel assemblies and four types of fuel (see Figure 1 (b)), and its main aspects are presented in Table 1.

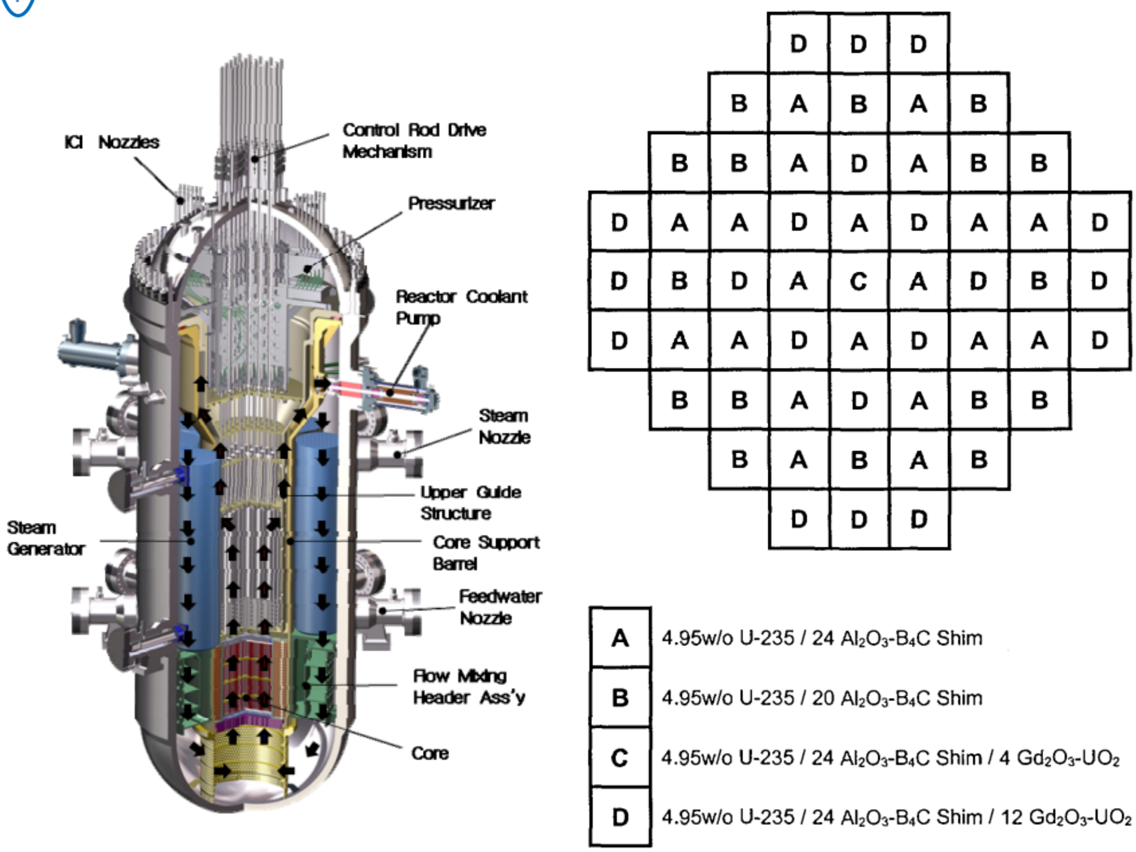

Figure 1. (a) SMART reactor pressure vessel and main components [5]. (b) Core fuel distribution and composition for 57 fuel assemblies [7].

Table 1. SMART reactor specifications [8] with material of fuel cladding altered to Zircaloy-4.

Parameters	Value
Reactor thermal capacity (MWth)	330
Power plant Electrical capacity (MWe)	100
Equivalent core diameter (m)	1.8316
Reactor operating pressure (MPa)	15
Primary coolant flow rate (kg/s)	2090
Core coolant inlet temperature (°C)	270
Core coolant outlet temperature (°C)	310
Active core height (cm)	200
Assembly pitch (cm)	21.504
Pin pitch (cm)	1.2598
Pellet radius of UO_2 fuel rod (cm)	0.3925
Stack height density of UO_2 fuel rod (g/cm^3)	10.286
Inner radius of fuel cladding (cm)	0.41875
Outer radius of fuel cladding (cm)	0.475
Material of fuel cladding	Zircaloy-4
Pellet radius of Gd_2O_3+UO_2 fuel rod (cm)	0.4066
Material of control rod	Ag–In–Cd
Total height of reactor vessel (m)	12.5

The passive safety features are part of the preventive measures against major loss of coolant accidents (LOCA) and include effective control systems that preserve the core structure. However, natural operational damage, unexpected malfunctions, or human errors may still initiate accidents. [9]. In this sense, this paper investigates the loss of flow accident (LOFA), which is among the most severe accidents that may occur during a reactor's operation [10].

2. METHODOLOGY

The RELAP5-MOD3.3 code [11] was used to simulate the steady-state operation of the SMART core, followed by a LOFA transient. A total of 57 heat structures and thermal hydraulic channels (THC) subdivided into 10 axial levels were used to simulate the fuel assemblies and coolant flow in the core (see Figure 2 for a schematic representation).

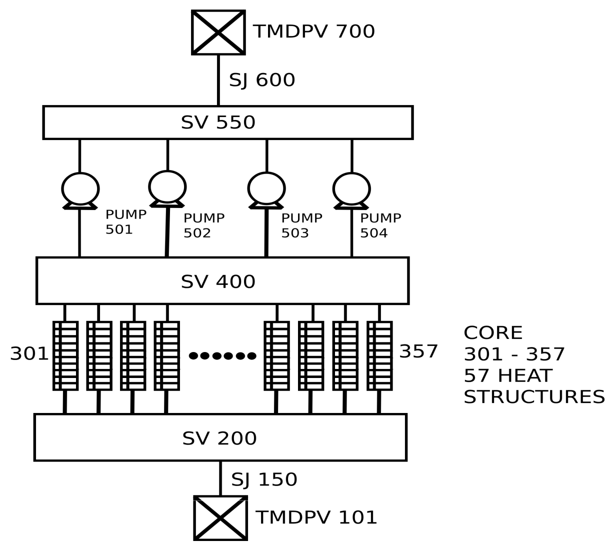

Figure 2. Core nodalization using the RELAP5 code. SJ: single junction; SV: single volume; TMDPV: time dependent volume.

To simulate crossflow and obtain a more realistic flow redistribution in a LOFA scenario, a total of 140 single junctions were used in odd levels of selected thermal hydraulic channels (see right side of Figure 3). The code was allowed to run for 1000 s, with the blockage of the A15, A8 and D11 channels occurring at 150 s, 300 s and 450 s, respectively.
The selection of the cited channels was based on the inlet mass flow distribution in the core, presented in data from the SCOP facility (SMART COre flow distribution and Pressure drop test) [12], and the ideal power distribution of the fuel assemblies at the beginning of cycle and hot full power, present in the the conceptual design of the reactor [7]. From these data, it can be noted that the fuel elements in positions A8 and A16 have high mass flow and predicted power (see left side of Figure 3 and the conceptual design), making them more susceptible to cladding deformations and deterioration. These factors may produce long-term operational problems that could require human intervention, both of which could result in unexpected errors and a subsequent reduction in the coolant flow. The element D11 was blocked due to its positioning between A8 and A15, which produces a more extreme blockage scenario.

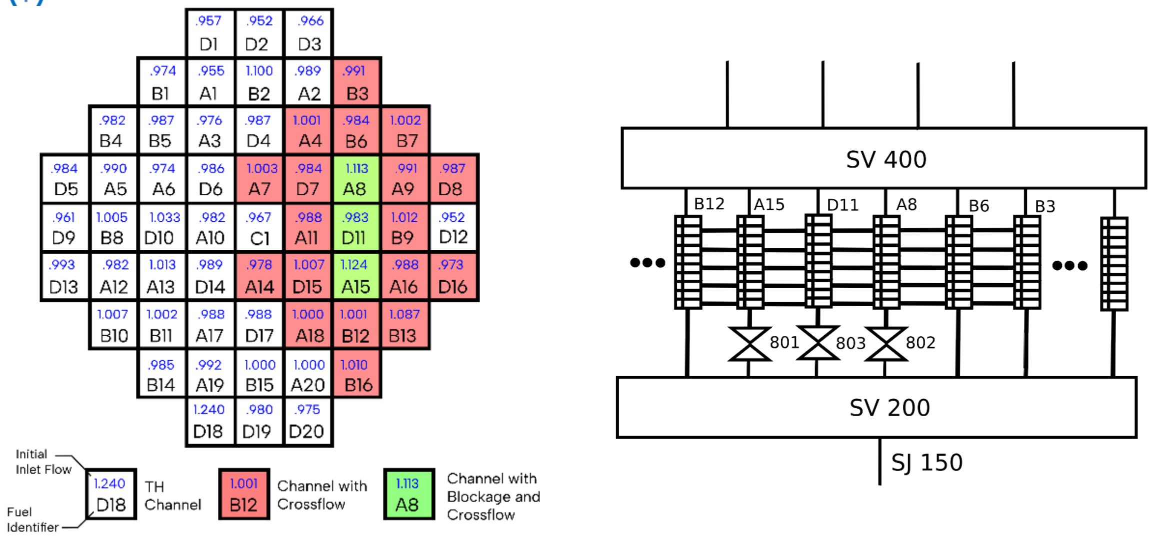

Figure 3. THCs in the nodalization of the core (left) and the valves inserted for the LOFA simulation (right).

3. RESULTS

3.1. Steady-State

The model verification can be achieved by comparing the simulation results under steady-state conditions with corresponding values from the literature (see Table 1). Table 2 presents some key parameters and their difference from reference values.

Table 2. Steady-state results obtained from RELAP5 simulation.

Parameter	**Reference** [8]	**Calculated**	**Calculated/Acceptable Error (%)** [13]
Reactor operating pressure (MPa)	15	14.96	0.3/-
Primary coolant flow rate (kg/s)	2090	2088.68	0.06/2
Core coolant inlet temperature (°C)	270	269.99	$\sim$ 0/0.5
Core coolant outlet temperature (°C)	310	310.32	0.1/0.5

The errors obtained in the simulation are within the acceptable range and, thus, demonstrates the agreement between the model used and the expected hydrodynamic operation of the reactor. The local pressure drop observed was of 530 kPa.

3.2. Transient

The transient simulation was characterized by the blockage of the THCs A8, A16 and D11 (see Figure 4 (a)). As expected, the cross flow prevented the mass flow rate from falling too low (see Figure 4 (b)) and is exemplified at Figure 4 (c), where the negative values is due to the orientation of the junction. Overall, the second graph shows that the mass flow increased in channels without crossflow, which is foreseen as the valve lock forces the coolant to be redistributed. Nevertheless, the THC connected to the blocked ones lose more coolant than they gain to compensate for the blockage, hence the decrease in their total mass flow.

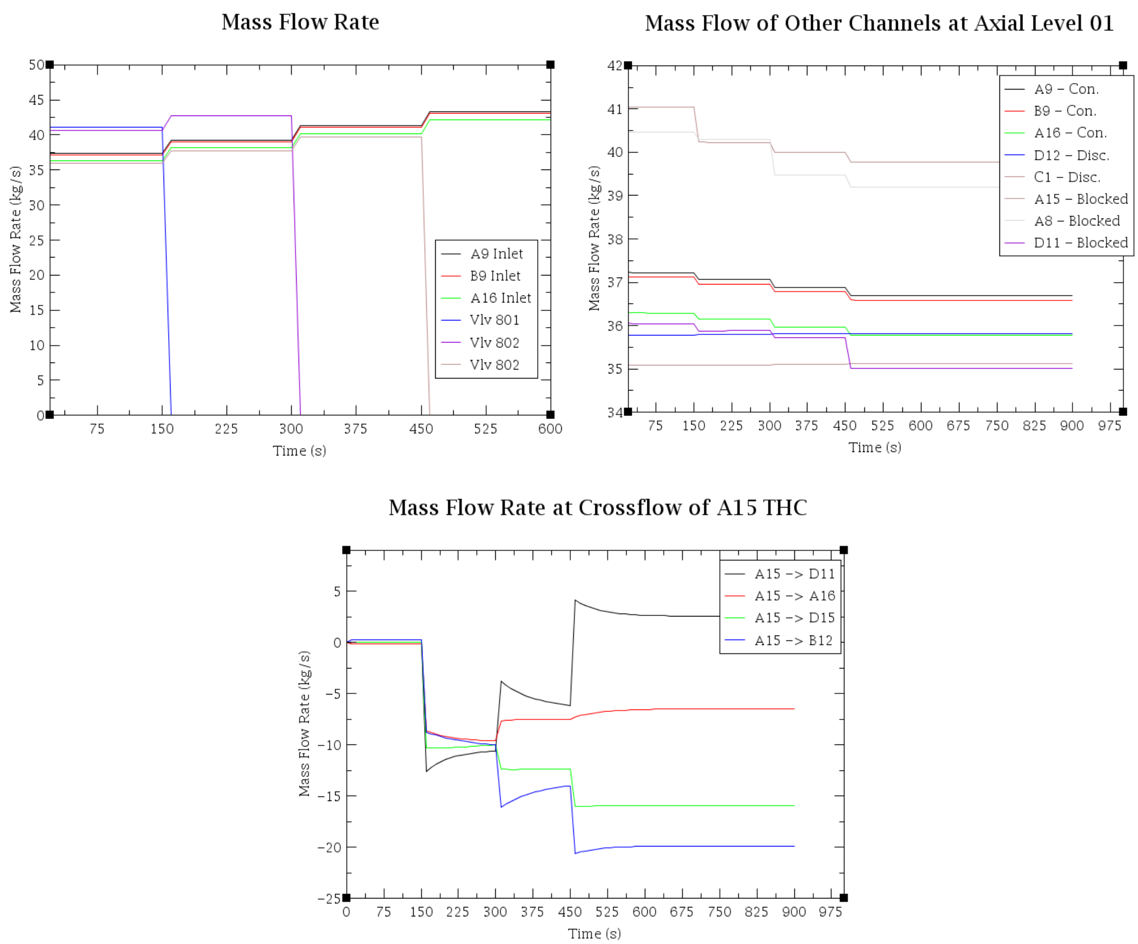

Figure 4. (a) Mass flow rate at valves and inlet of the channels blocked; (b) Mass flow variation of selected channels, where "Con." indicates that the channel has crossflow and "Disc." indicates its absence; (c) mass flow at the axial level 01 crossflow junction of A15 THC; the arrows indicate the orientation of the junction.

Figure 5 demonstrates the coolant temperature increase of about $\sim 1\%$ at the blocked THCs and of negligible amounts at the core inlet and outlet increased (see Figure 5), as predicted, but neither reached the saturation temperature of $T_{sat} = 612.49\ K$ and, thus, there was no production of water steam inside the channels. Surrounding channels experienced similar effects, but were significantly smaller due to the cross flow.

Furthermore, an increase of the fuel temperature was also observed (see Figure 6 (a)), where the maximal fluctuation was of $\sim 20\ K$. This effect is a natural consequence of the higher coolant temperature, which decreases the heat transfer from the cladding given the smaller temperature difference between the former and the latter. On the other hand, the inlet and outlet pressure did not

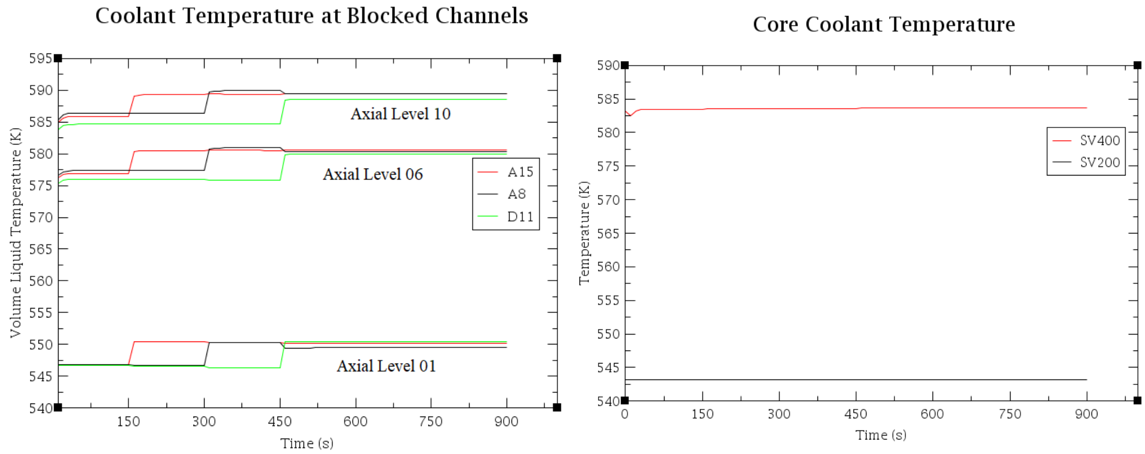

Figure 5. Coolant temperature at the blocked THCs (a) and at the core inlet and outlet (b).

experience significant changes after the valves lock (see Figure 6 (b)). This is a desirable result, as the ideal pressure drop of the steady-state is preserved. In any case, the fuel remained in safe temperature ranges [14] in all axial levels.

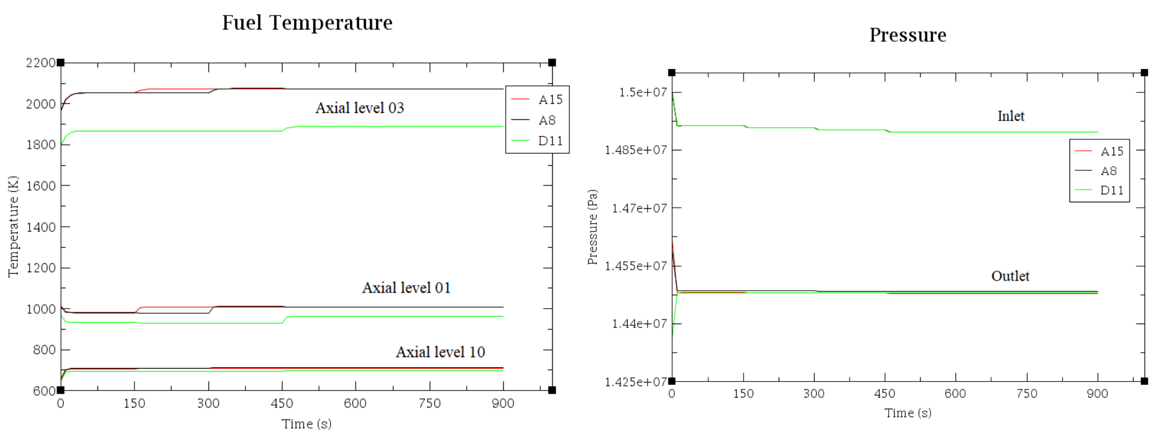

Figure 6. (a) Fuel temperature at different axial levels and (b) pressure at the inlet and outlet for the three blocked channels.

In general, the results show that the LOFA did not produce severe effects on the key parameters of the core or individual THCs.

3.2.1. Channel Blockage without Crossflow

To demonstrate the importance of the crossflow in a nuclear reactor modeling, the removal of the crossflows of the TH channel D11 was considered. Figure 7 presents the resulting mass flow rate and fuel temperature at the axial level with highest power. The code calculation stopped at $t \approx 470.7\ s$ due to the general extrapolation of the fuel temperature, which surpassed 3000 K. The cladding was also heated to above 2800 K. These results demonstrate the fuel centerline melting due to the temperature limits of the cladding material (Zircaloy-4) being reached [14].

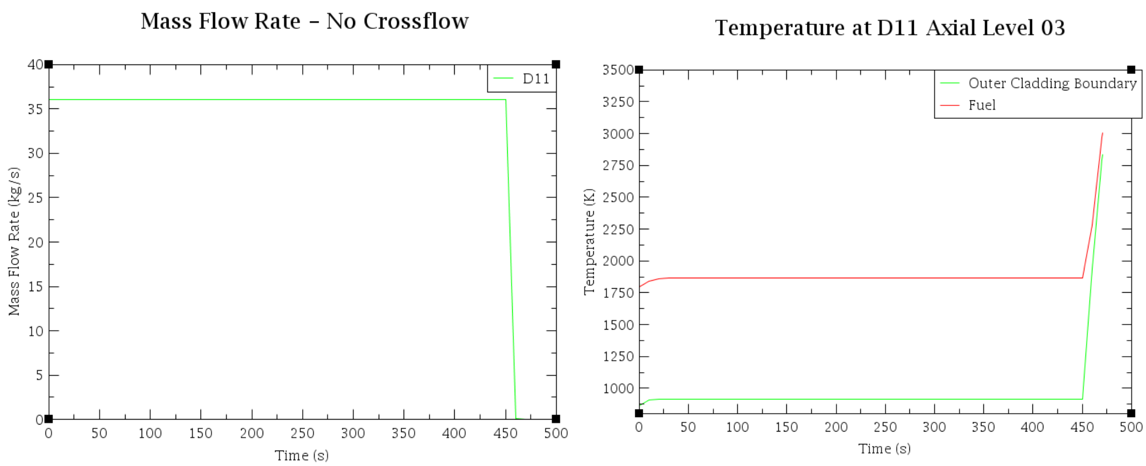

Figure 7. (a) Mass flow time evolution and (b) fuel temperature at axial level 03 of the THC D11 without crossflow.

4. CONCLUSION

The modeling of the SMART core using the RELAP5/MOD3.3 code was evaluated. The expected steady-state values presented in Table 1 were verified and the errors of the calculation (Table 2) were within acceptable limits. From this point, a LOFA scenario was simulated by a transient characterized by channel blockages in the elements A16, A8 and D11, which were selected for being sensitive points of the core.

From Figure 4 and Figure 6, the effects of the LOFA scenario were observed to be minimal, with the operation of the selected channels not being significantly affected. In fact, the coolant temperature variations were not high enough for concerns as it remained distant from the saturation temperature of $T_{sat} = 612.49\,K$. Moreover, the highest fuel temperature fluctuation was of $\sim 20\,K$ (axial level 03 of A8 and A15), which corresponds to a variation of around 1% of their original temperatures. The pressure also did not vary significantly.

Lastly, Figure 5 shows the absence of noticeable fluctuations in key parameters, further supporting that the LOFA did not cause considerable damage to the core and its functioning. Contrariwise, Figure 7 demonstrates the problematic results of a simulation without the use of crossflow, as the fuel and cladding temperature surpassed the temperature limits of the materials, hence showing that the use of cross flow in modeling is essential to more realistically reproduce the core behavior and simulate channel blockage transients.

The results obtained verified the thermal hydraulic safety of the model developed for the SMART reactor and demonstrated that a LOFA is not sufficient to cause great core damage or reduce operational capacity. The simplicity of the primary coolant system, however, highlights the limitations of the model, which demands an expansion to account for more nuanced mechanisms, such as the continuous flow in a loop and thermal interactions with the steam generator.

ACKNOWLEDGEMENTS

The authors are grateful to the Brazilian research funding agencies: Coordenação de Aperfeiçoamento de Pessoal de Nível Superior (CAPES), Fundação de Amparo à Pesquisa do Estado de Minas Gerais (FAPEMIG) and Conselho Nacional de Desenvolvimento Científico e Tecnológico (CNPq) for the support.

References

[1] E. M. Hussein, "Emerging small modular nuclear power reactors: A critical review", *Physics Open*, vol. 5, p. 100 038, 2020, issn: 2666-0326. doi: `https://doi.org/10.1016/j.physo.2020.100038`.

[2] M. K. Rowinski, T. J. White, and J. Zhao, "Small and medium sized reactors (smr): A review of technology", *Renewable and Sustainable Energy Reviews*, vol. 44, pp. 643–656, 2015, issn: 1364-0321. doi: `https://doi.org/10.1016/j.rser.2015.01.006`.

[3] R. o. KAERI (Korea, "System-integrated modular advanced reactor (smart)", International Atomic Energy Agency, IAEA-TECDOC 1485, 2006.

[4] International Atomic Energy Agency, "System-integrated modular advanced reactor (smart)", in *Status of Innovative Small and Medium Sized Reactor Designs 2005: Reactors with Conventional Refuelling Schemes* (IAEA-TECDOC-1485), IAEA-TECDOC-1485. Vienna, Austria: International Atomic Energy Agency, 2006, pp. 93–116, isbn: 92–0–101006–0.

[5] K. K. Kim, W. Lee, S. Choi, H. R. Kim, and J. Ha, "Smart: The first licensed advanced integral reactor", *Journal of Energy and Power Engineering*, vol. 8, pp. 94–102, 2014.

[6] J. Yoon, S. Y. Ryu, B. S. Choi, M. Lee, and S. K. Zee, "Plant system design features of smart", in *GENES4/ANP2003*, Korea Atomic Energy Research Institute (KAERI), Kyoto, JAPAN, Sep. 2003, Paper 1049.

[7] J. Park, "Nuclear characteristics analysis report for system-integrated modular advanced reactor (smart)", Korea Atomic Energy Research Institute, Tech. Rep. KAERI/TR-1162/98, 1998.

[8] A. Pourrostam, S. Talebi, and O. Safarzadeh, "Core analysis of accident tolerant fuel cladding for smart reactor under normal operation and rod ejection accident using dragon and parcs", *Nuclear Engineering and Technology*, vol. 53, no. 3, pp. 741–751, 2021, issn: 1738-5733. doi: `https://doi.org/10.1016/j.net.2020.08.025`.

[9] International Atomic Energy Agency, *Safety Analysis for Research Reactors* (Safety Reports Series No. 55). Vienna, Austria: International Atomic Energy Agency, 2008.

[10] C. Suresh, G. Sateesh, S. K. Das, S. Venkateshan, and M. Rajan, "Heat transfer from a totally blocked fuel subassembly of a liquid metal fast breeder reactor: Part i. experimental investigation", *Nuclear Engineering and Design*, vol. 235, pp. 885–895, 2005.

[11] C. D. Fletcher and R. R. Schultz, "Relap5/mod3 code manual", Jan. 1992. [Online]. Available: `https://www.osti.gov/biblio/5559769`.

[12] D. J. Eo, Y. J. Yoon, J. W. Lee, *et al.*, "Smart reactor flow distribution test (scop-e-01)", Korea Atomic Energy Research Institute, Tech. Rep. KAERI/TR-4224/2010, 2010.

[13] A. Petruzzi and F. D′Auria, "Thermal-hydraulic system codes in nulcear reactor safety and qualification procedures", *Science and Technology of Nuclear Installations*, vol. 2008, no. 1, p. 460 795, 2008. doi: `https://doi.org/10.1155/2008/460795`.

[14] P. A. Reis, I. R. Magalhães, R. B. de Faria, *et al.*, "Accident tolerant fuels behavior analysis for pressurized water reactor in steady state and transient conditions", *Nuclear Engineering and Design*, vol. 415, p. 112 673, 2023, issn: 0029-5493. doi: `https://doi.org/10.1016/j.nucengdes.2023.112673`.